AIAA 2000-0677

Inviscid Design of Hypersonic Wind Tunnel Nozzles for a Real Gas

J. J. Korte
NASA Langley Research Center
Hampton, Virginia

38th Aerospace Sciences Meeting & Exhibit
10-13 January 2000 / Reno, NV

INVISCID DESIGN OF HYPERSONIC WIND TUNNEL NOZZLES FOR A REAL GAS

J. J. Korte*

NASA Langley Research Center, Hampton, Virginia 23681

Abstract

A straightforward procedure has been developed to quickly determine an inviscid design of a hypersonic wind tunnel nozzle when the test gas is both calorically and thermally imperfect. This real gas procedure divides the nozzle into four distinct parts: subsonic, throat to conical, conical, and turning flow regions. The design process is greatly simplified by treating the imperfect gas effects only in the source flow region. This simplification can be justified for a large class of hypersonic wind tunnel nozzle design problems. The final nozzle design is obtained either by doing a classical boundary layer correction or by using this inviscid design as the starting point for a viscous design optimization based on computational fluid dynamics. An example of a real gas nozzle design is used to illustrate the method. The accuracy of the real gas design procedure is shown to compare favorably with an ideal gas design based on computed flow field solutions.

Nomenclature

C_1	= constant in Eq. (1)
C_d	= contraction coefficient
M	= Mach number
r^*	= nozzle throat radius or height
R_c	= throat radius of curvature/r^*
S	= $R_c + 1$
x	= axial coordinate
X_a	= start of subsonic contour with Eq.(1)
y	= radial coordinate
y_w	= nozzle wall radial coordinate
y_w'	= nozzle wall slope
γ	= gamma, ratio of specific heats
θ_a	= subsonic approach angle
θ_{super}	= nozzle inflection angle

Introduction

A number of hypersonic wind tunnel facilities have required new wind tunnel nozzles either to replace existing nozzles or to extend the facility capabilities into new flight regimes. These changes have been driven in part by the effort to develop a viable scramjet engine for hypersonic vehicles and for access-to-space initiatives. To simulate this type of vehicle and engine environment at hypersonic velocities requires stagnation conditions where the test gas typically behaves both as calorically and thermally imperfect through part of or the entire

nozzle. The inviscid design of a supersonic (and hypersonic) wind tunnel nozzle for a perfect gas was originated by Busseman in the 1920s (as noted in Ref. 1) and, in the opinion of the author, was finally perfected by Sivells[2] in the 1960s. No similar progress has been made for real gas wind tunnel nozzle design. This paper concentrates on an approximate inviscid nozzle design process for a calorically and thermally imperfect test gas.

Supersonic Wind Tunnel Nozzle Design

Ideal Gas Design

The theory used in the design of supersonic wind tunnel nozzles for an ideal gas can be found in a number of reports[3-6] and books.[7-9] The basic assumption made is that the boundary layer thickness is small compared to the characteristic length (nozzle radius), so the nozzle flow field can be treated as inviscid for designing the aerodynamic lines. Once the aerodynamic lines are determined, a correction is made to account for the displacement thickness of the boundary layer. This basic procedure has been applied successfully to many supersonic and hypersonic nozzles. A computational fluid dynamics (CFD) analysis should then be made to validate the flow quality and the design Mach number for the nozzle design. If the desired flow quality or Mach number is not obtained, this failure usually means that the boundary layer assumption was invalid and a different design method, which directly includes the viscous effects should be used.[10]
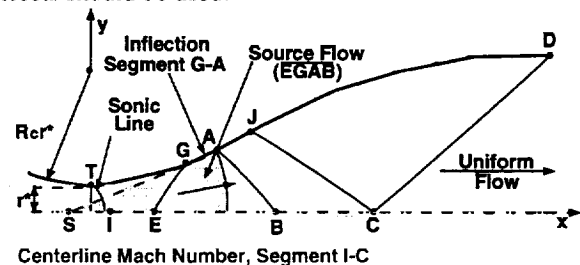

Fig. 1 Wind tunnel nozzle flow regions.

The classical inviscid design procedure requires the position of the sonic line at the throat, a prescribed centerline Mach number, and the condition of uniform flow at the nozzle exit (Fig. 1). Sivells[2] determined the appropriate centerline Mach number distribution that would result in a nozzle wall with continuous wall slope and curvature from the throat to the exit. The centerline Mach number distribution for the upstream and turning sections is based on polynomial functions that match the

*Senior Research Engineer, Multidisciplinary Optimization Branch, Mail Stop 159, Senior Member AIAA.

flow field solutions at each flow region boundary. This distribution results in a wall contour shape that is easier to machine.

Once a centerline Mach number distribution has been specified, the classical design procedures use an inverse method-of-characteristics (MOC) design procedure to determine an inviscid contour. This inviscid contour can then be scaled to any particular size. The design contour for one operating condition is determined by computing the displacement thickness by using a boundary layer (BL) code and adding it to the inviscid contour. Modern implementations of MOC-BL design procedures typically differ in the way the sonic line and centerline Mach number distributions are specified and in the numerical techniques used to compute the inviscid flow field and the boundary layer solution.

Real Gas Design

Real gas effects are important in the design of many hypersonic blow down and reflected shock facilities. Recent advances in wind tunnel nozzle design with CFD codes coupled to optimization techniques[11] or with traditional MOC-BL design procedures are two options for designing a nozzle. A CFD-based method is the more accurate design procedure when the boundary layer is extremely thick.[10] However, for reflected shock tunnels, the run time is short enough that the nozzle wall stays cold, and the boundary layer is thin enough that accurate designs can be obtained with the classic MOC-BL approach. The CFD solutions for the reflected shock nozzles are extremely time-consuming due to the fine grid requirements for accurately simulating the thin nozzle boundary layers.

At least two approaches have been used to include real gas effects in an MOC design procedure. The first approach is to include real gas behavior by using tabulated thermodynamic properties, assuming a thermally perfect gas.[12] The second approach is to divide the nozzle into flow regions, which include a source flow region where the source flow is computed with a one-dimensional real gas code and is connected to a turning contour computed with an MOC design procedure for a calorically perfect or imperfect gas.[13,14] Neither method addresses high pressure effects nor exploits a centerline Mach number distribution which guarantees a nozzle wall with continuous wall curvature. Both designs methods start with a source flow region at the nozzle throat.

A variation of the second approach is used to develop a design procedure applicable to a real test gas with both caloric and thermal imperfections that would produce a wall design with continuous wall curvature. The method described in this paper differs from previous methods in that the approach follows Sivells' design philosophy of prescribing a centerline Mach number distribution and includes high pressure effects in the throat region. The author has successfully used this method to design a number of hypersonic wind tunnel nozzles at NASA Langley Research Center and elsewhere.[15]

Procedure for Real Gas Inviscid Hypersonic Nozzle Design

The design procedure will be described assuming that the nozzle will have an axisymmetric geometry. The process and the computer codes developed can also handle two-dimensional nozzle design. The inviscid contour design is obtained by dividing the nozzle into four sections: (1) subsonic and throat section, (2) throat to conical section, (3) conical or source flow section, and (4) turning contour downstream of the conical section. Five specific steps are used to design the complete inviscid contour. For describing the design method, we will assume that the throat radius, throat radius of curvature ratio, stagnation conditions, compressibility factor, specific heats ratio (gamma), and gas composition are known. (Sometimes the exit diameter is given and the throat radius needs to be determined.)

The first four steps will be completed with coordinates made nondimensional by the throat radius. The final design is obtained by scaling the nozzle design to obtain the desired throat radius or exit radius.

The procedure will be explained and demonstrated with various options in Sivells' design code[16] for designing the inviscid contour of nozzle sections. In addition, an approach for defining a centerline Mach number distribution for use in a CFD-based design process will also be described.

Once the inviscid design is completed, a BL code (like Anderson's)[17] can be used to correct the nozzle for the displacement thickness, assuming turbulent flow and chemical and vibrational equilibrium. The nozzle design can then be validated with computed CFD solutions by using the procedure and the codes described by Korte.[18] Typically the final nozzle contour length will be determined by truncating the nozzle design based on the boundary layer growth observed in the CFD flow field solutions or from facility length restrictions.
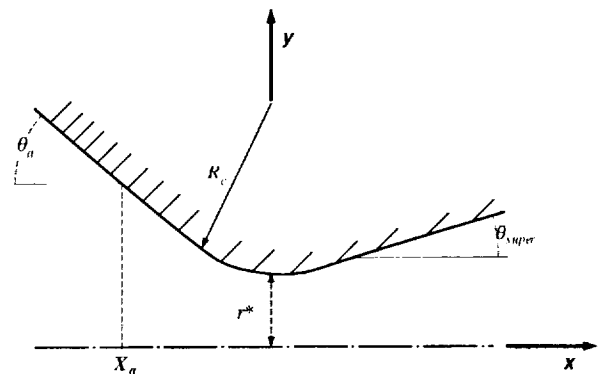

Fig. 2 Subsonic and transonic nozzle geometry.

Step 1: Subsonic-Throat Region

The geometry of a continuous curvature throat section used in the design method is given in Fig. 2. To connect the subsonic side of the throat section to an entrance cone or wedge, the subsonic contour was specified by the equation[19]

$$y_w / r^* = C_1\left[1 - \exp\left(-(x/r^*)^2/(2C_1R_c)\right)\right] + 1 \qquad (1)$$

where

$$C_1 = R_c \tan^2(\theta_a)\exp(1) \qquad (2)$$

and the point of intersection with the entrance cone or wedge is

$$X_a / r^* = -R_c \tan(\theta_a)\sqrt{\exp(1)}. \qquad (3)$$

This subsonic contour has the desirable qualities of providing an exponential decay of the curvature away from the throat into a cone (or wedge) inlet and approaching the throat similar to a contour described by a circle.

Step 2: Real Gas Geometric Area Ratio

The second step is to determine the real gas area ratio for the design conditions. A steady, quasi-one-dimensional flow field solution that includes all real gas effects is needed. This solution can be obtained by either solving the steady-state equations directly for a given Mach number[20] or by using standard CFD techniques to compute the steady-state one-dimensional solution for an expanding source flow until the desired exit condition is obtained.

Once the one-dimensional solution for the area ratio has been determined, the geometric area ratio for the nozzle must be computed. The curvature of the nozzle in the throat region introduces a contraction effect due to the curvature of the sonic line. Compared to a one-dimensional calculation, the contraction effect reduces the mass flow through the throat. Sivells' contraction coefficient is computed by using an expansion solution for the transonic flow region.[16] For an axisymmetric flow

$$C_D = 1 - \frac{\gamma+1}{96S^2}\left[1 + \frac{8\gamma-2}{24S} + \frac{75\gamma^2 - 757\gamma + 3615}{2880S^2} + ...\right] \qquad (4)$$

The geometric area ratio is calculated by multiplying the one-dimensional area ratio and the contraction coefficient.

Step 3: Throat to Conical Section Design

The third step is to determine the contour design from the throat to the beginning of the conical section using Sivells' MOC design code. The necessary input parameters define the centerline Mach number distribution for the MOC design. The input parameters are defined by the ratio of the radius of curvature to the throat radius, expansion angle, ratio of specific heats, and by specifying the Mach numbers at points B and C in Fig. 1. To facilitate the final step, we select Sivells' option for including points along the source flow section and choose the axial coordinate to be measured from the upstream source for the radial flow region. The gamma is selected to be the approximate value for the transonic region (Mach = 1.0 to 1.3) and the throat radius is specified to be unity. For most gases, the temperature change is limited in this range, resulting in only minor variations of gamma.

Step 4: Turning Contour Design

The next step is to design the contour downstream of the conical section by using Sivells' code for the gamma at or near the design Mach number. The same inputs to Sivells' code are used except that the gamma is changed and the nozzle exit diameter is specified to achieve the geometric area ratio obtained in step 2.

Step 5: Assembling the Inviscid Nozzle Design

The final step of the inviscid design is to assemble the pieces. First the throat-to-end of the conical section (step 3) is combined with the turning contour design (step 4). Usually a portion of the conical section obtained from the throat-to-conical section design overlaps the turning contour design. The overlap portion is removed, slightly reducing the size of the conical flow region obtained in step 3. Next the origin of the axial coordinates is transformed from the origin of the source to the nozzle throat. Now the subsonic-throat region (step 1) can be added directly to the rest of the design. The final design coordinates are obtained by scaling both coordinates by a common factor to obtain either the desired throat or exit radius.

Limits of Design Procedure

The above procedure assumes that the design parameters selected for the nozzle will result in a conical (source) flow region. This can usually be accomplished by selecting the appropriate expansion angle. If the first choice of expansion angle results in a nozzle design without a conical section, the expansion angle can be lowered until a reasonable design is obtained. Typically, this problem occurs only in low supersonic nozzle designs. This procedure also assumes that the gamma will increase (or stay constant) as the flow expands.

Centerline Mach Number Distribution for Use with CFD-Based Design Codes or Real Gas MOC Design Codes

The above procedure was illustrated with the assumption that Sivells' computer code was being used to design the different supersonic parts of the nozzle contour. There are a few applications where a real gas MOC design code or a CFD-based design procedure must be used because of either rapidly varying gamma effects in the turning region or the BL size. A centerline Mach number distribution needs to be prescribed either as a boundary condition or as part of the objective function. A centerline Mach number distribution for use in the design can be determined by using a similar approach as Sivells.

The advantage of Sivells' centerline distribution is that it smoothly matches the different flow regions, eliminating discontinuities in contour curvature. In Sivells' method, the centerline distribution consisted of four sections: (1) a fourth-order polynomial connecting the transonic section and the source flow regime, (2) the source flow region, (3) a fifth-order polynomial connecting the source flow region and the uniform flow regime, and (4) the uniform flow region at the design

Mach number. The coefficients of the polynomials are determined by matching the Mach number or axial velocity and its derivatives, with respect to nozzle length, at the beginning and end of each section. Sivells derived for the ideal gas equations the Mach number derivatives with respect to the area ratio for the source flow region and the nozzle sonic line. For a real gas, the coefficients of the polynomials and the source flow region need to be computed with a real gas model.

The necessary data for the source flow and the polynomial coefficients can easily be computed with two different CFD flow field solutions. The first CFD solution is for a two-dimensional (or axisymmetric) flow field in the subsonic-transonic region of the nozzle. The subsonic contour is defined by Eq. (1) and the supersonic side can be described using any expansion that preserves continuity at the throat wall in radius, slope, and curvature. Because the inviscid supersonic flow field is hyperbolic, the supersonic flow field does not affect the solution at the sonic line. The throat contraction coefficient and the derivatives of Mach number and axial velocity at the throat can then easily be computed from the flow field solution. This part of the procedure is already being used in the design method described by Korte et al.[11] The second solution needed is for a quasi-one-dimensional flow field to obtain the Mach number and its derivatives with respect to nozzle area ratio. This flow field solution is also needed to define the area ratio of the nozzle, as described in the section above. A future paper will present results for an optimized nozzle design that uses CFD-based techniques with an objective function for the centerline Mach number as defined in this paragraph.

Application and Accuracy of the Design Procedure

An example of the nozzle design process will be given in this section, along with computed inviscid CFD flow fields to validate the design process. Two nozzles will be designed, analyzed, and compared for flow quality. The nozzles will be designed with the same parameters except that the ratios of specific heats will be different to account for different gas assumptions.

One nozzle will be designed for an ideal gas by using Sivells' design code with a gamma computed to give the design Mach number at the same area ratio as the real gas design. The other case will use the real gas procedure for a calorically and thermally imperfect gas. The same parameters will be used for defining the centerline Mach number distribution, except for the ratio of specific heats. The flow quality of the nozzle designs will be evaluated based on the CFD inviscid simulations.

Nozzle Design

To demonstrate the procedure, we will design a nozzle for an exit Mach number of 14, with stagnation conditions that have significant real gas effects. These specifications are made based on the availability of a validated real gas equation of state for high pressure and temperature nitrogen from previous work.[18]

For the flow conditions given in Table 1, the one-dimensional real gas area ratio is computed to be 2396.87. If only caloric imperfections are considered, then the area ratio is computed to be 3232.44. The ratio of specific heats (γ) for an ideal gas needed to obtain Mach 14 and an area ratio of 2396.87 is 1.4073. If the test gas is air and it is treated as an ideal gas, the area ratio for Mach 14 with $\gamma = 1.4$ is 2686. The nonideal effects of the high pressure (on the thermal equation of state) and the high temperature (on the caloric equation of state) offset each other so that the real gas area ratio is only 10.8% lower than the ideal gas area ratio for $\gamma = 1.4$.

Table 1. Nozzle design conditions and parameters

Total pressure	20,000 psi
Total temperature	3,000°R
Gas composition	Nitrogen
Stagnation compressibility factor	1.31205
Exit Mach number	14.0
Subsonic approach angle	45°
Ratio radius-of-curvature/throat radius	3.0
Supersonic (source flow) angle	12.0°
Throat radius	1.0
Geometry	Axisymmetric

Table 2. Area ratios and ratio of specific heats

Case	Gas model	Mach	γ	Area ratio
1	Real gas	1.0	1.3180	
"	"	1.3	1.3234	
"	"	14.0	1.4000	2396.87*
2	Ideal gas	14.0	1.4073	2396.87

*For conditions given in Table 1.

Two nozzles were designed for the specifications given in Tables 1 and 2. The input for Sivells' code for each case is given in the appendix Table A1. The real gas area ratio is computed with a real gas equation of state for nitrogen. The ideal gas nozzle design is only for comparing flow quality with that of the real gas design. The subsonic contour is identical for both nozzle designs (appendix, Table A2). The supersonic contours for both nozzles are given in appendix Table A3.

CFD Analysis of Nozzle Design

A CFD flow field solution for each nozzle was computed by using the methods given in Refs. 11 and 18. Both the designs and the CFD analyses used the same equation of state. The throat region was computed by solving the unsteady Euler equations. The throat numerical grid was 81 × 75 points in the axial and normal directions, respectively. The centerline solution for the throat started at approximately Mach 0.2 and ended at approximately Mach 1.8. The downstream portion of the nozzle was computed by solving the steady Euler

equations with a space marching method and was computed in approximately 1000 marching steps.

The computed centerline Mach number distributions for the whole nozzle in each case are compared in Fig. 3.
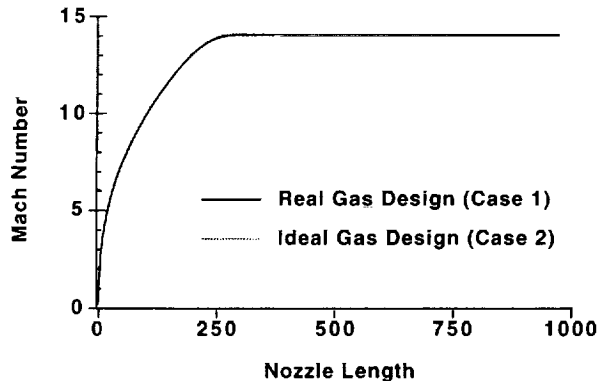

Fig. 3   Comparison of computed centerline Mach number distributions for real and ideal gas nozzle designs.

At this scale there are no differences in the two designs, and both appear to generate the ideal uniform core region at Mach 14. Focusing in on the uniform core region in Fig. 4 shows slight Mach number variations on the order of 0.02 Mach for each case.
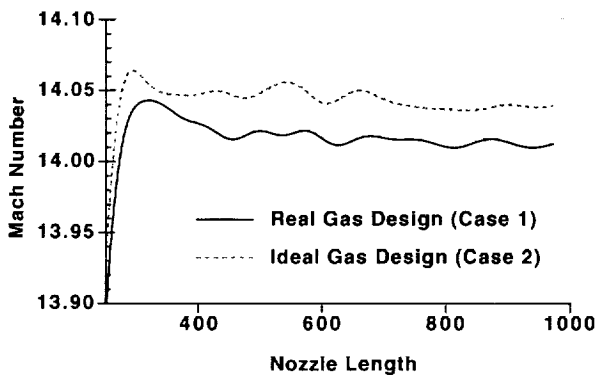

Fig. 4   Comparison of computed centerline Mach number distributions for real and ideal gas nozzle designs in uniform core region.
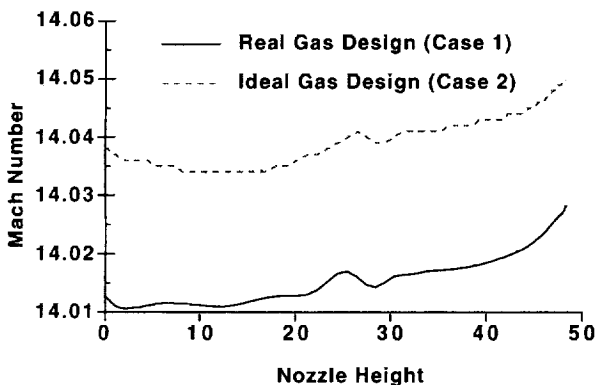
Fig. 5 Comparison of exit Mach number profile for real and ideal gas nozzle designs.
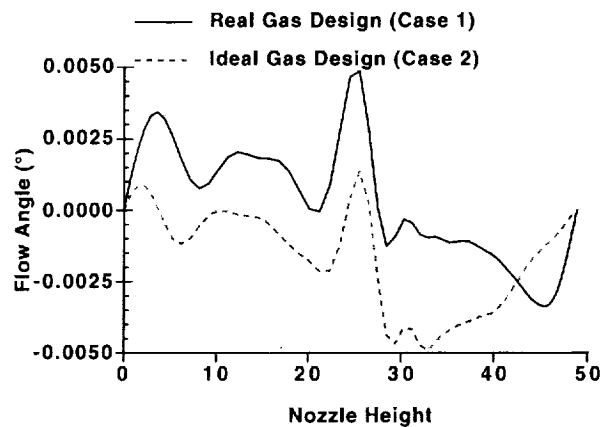
Fig. 6 Comparison of exit flow angle profile for real and ideal gas nozzle designs.

The exit Mach number profiles are given in Fig. 5, and the angle profiles are given in Fig. 6. The flow is essentially uniform at both nozzle exits because the magnitude of the flow angles is so small. The Mach number profile at the exit varies approximately 0.02 Mach across the nozzle height. The computed exit Mach numbers for both nozzles were slightly higher than the Mach 14 design point: Mach 14.04 for the ideal gas design and Mach 14.02 for the real gas design. This minor variation from the design point is most likely due to the differences in the transonic expansion solution for the nozzle throat used in the design. Mach contours for the real gas nozzle design shown in Fig. 7 show only a 0.01 Mach number variation in the uniform core region.
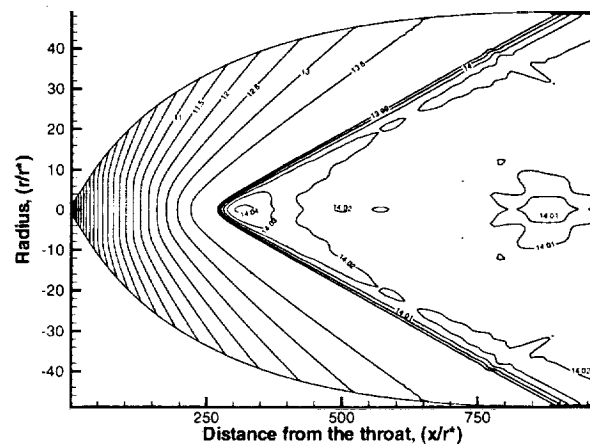
Fig. 7   Computed Mach contours for a real gas nozzle design.

In both designs, minor variations from the Mach 14 design point are observed. However, the variations are similar and are most likely characteristic of Sivells' design process, not of the real gas design procedure presented above. In fact, the computed solution for the real gas nozzle has flow quality almost identical to that of the computed ideal gas nozzle design. Variations of this real gas design procedure have been used to design

5
American Institute of Aeronautics and Astronautics

nozzles at Langley and elsewhere with excellent results.[15,21]

Summary

A simple, straightforward method for the inviscid design of a real gas nozzle for hypersonic facilities has been proposed. The design is demonstrated for real gas conditions with significant calorically and thermally imperfect effects. An ideal gas nozzle is also designed for the same area ratio and Mach number for comparison of flow quality. CFD flow field solutions are computed for each nozzle, and the flow field qualities in terms of Mach number variation and flow angle are compared. The nozzle designs have nearly identical computed flow quality. This method is easy to use and is extremely accurate when the real gas effects occur before the beginning of the turning contour design.

References

[1]Anderson, J. D., *Modern Compressible Flow*, 1st ed., McGraw-Hill, New York, 1982, pp. 303-305.

[2]Sivells, J. C., "Aerodynamic Design of Axisymmetric Hypersonic Wind Tunnel Nozzles," *Journal of Spacecraft and Rockets*, Vol. 7, Nov. 1970, pp. 1292-1299.

[3]Armstrong, A. H., and Smith, M. G., "Two-Dimensional Supersonic Nozzle Design, Part I: Theory," Armament Research Establishment, Report No. 5/51, Oct. 1951.

[4]Ruptash, J., "Supersonic Wind Tunnels-Theory, Design and Performance," University of Toronto, Institute of Aerophysics, June 1952.

[5]Beckwith, I. E., and Moore, J. A., "An Accurate and Rapid Method for the Design of Supersonic Nozzles," NACA TN 3322, Feb. 1955.

[6]Johnson, C. B., "Real-Gas Effects on Hypersonic Nozzle Contours With a Method of Calculation," NASA TN D-1622, 1963.

[7]Lukasiewicz, J., *Experimental Methods of Hypersonics, Gasdynamics, Vol. 3, Part 1*, Dekker, New York, 1973, pp. 80-86.

[8]Zucrow, M. J., and Hoffman, J. D., *Gas Dynamics, Volume 2: Multidimensional Flow*, John Wiley & Sons, Inc., New York, 1977.

[9]Shapiro, A. H., *The Dynamics and Thermodynamics of Compressible Fluid Flow*, Vol. 1, The Ronald Press Company, New York, 1953.

[10]Korte, J. J., and Hodge, J. S., "Flow Quality of Hypersonic Wind-Tunnel Nozzles Designed Using Computational Fluid Dynamics," *Journal of Spacecraft and Rockets*, Vol. 32, No. 4, 1995, pp. 569-580.

[11]Korte, J. J., Kumar, A., Singh, D. J., and White, J. A., "CAN-DO, CFD-Based Aerodynamic Nozzle Design & Optimization Program for Supersonic/Hypersonic Wind Tunnels," AIAA Paper 92-4009, July 1992.

[12]Johnson, C. B., and Boney, L. R., "A Method for Calculating a Real-Gas Two-Dimensional Nozzle Contour Including the Effects of Gamma," NASA TM X-3243, 1975.

[13]Jacobs, P. A., and Stalker, R. J., "Design of Axisymmetric Nozzles for Reflected Shock Tunnels," Department of Mechanical Engineering, University of Queensland, Australia, Report 1/89, 1988.

[14]Hannemann, K., "Design of an Axisymmetric, Contoured Nozzle for the HEG," Institut für Theoretische Strömungsmechanik, DLR Report DLR-FB 90-04, Göttingen, Germany, 1990.

[15]Chadwick, K. M., Holden, M. S., Korte, J. J., and Anderson, E. C., "Design and Fabrication of a Mach 8 Contoured Nozzle for the LENS Facility," AIAA Paper 96-0585, Jan. 1996.

[16]Sivells, J. C., "A Computer Program for the Aerodynamic Design of Axisymmetric and Planar Nozzles for Supersonic and Hypersonic Wind Tunnels," AEDC-TR-78-63, Dec. 1978.

[17]Anderson, E. C., and Lewis, C. H., "Laminar or Turbulent Boundary-Layer Flows of Perfect Gases or Reacting Gas Mixtures in Chemical Equilibrium," NASA CR-1893, Oct. 1971.

[18]Korte, J. J., Hedlund, E., and Anandakrishnan, S., "A Comparison of Experimental Data With CFD For The NSWC Hypervelocity Wind Tunnel #9 Mach 14 Nozzle," AIAA Paper 92-4010, July 1992.

[19]Beckwith, I. E., personal communication, 1990.

[20]Eggers, A. J., Jr., "One-Dimensional Flows of an Imperfect Diatomic Gas," NACA Rep. 959, 1950.

[21]Gaffney, R. L. Jr., "CFD Calculations of the AHSTF Mach 6 Nozzle," to be published as Analytical Services and Materials Report, Hampton, VA.

Appendix

Table A1. Input data for Sivells' design code*

```
Case 1: Real gas design, upstream section-supersonic.
12345678901234567890123456789012345678901234567890123456789012345678901234567890
R_Gas-1          0
     1.323   1716.563      1.000      .896  0.227E-07       .000       .000   1000.000
    12.000      3.000       .000    11.200     14.000    .00000     -1.000     10.000
    41     21      0     10      1     41     49     61     32      0     -1     -1     10      0    -21     13
Case 1: Real gas design, downstream section-supersonic.
R_Gas-1          0
     1.400   1716.563      1.000      .896  0.227E-07       .000       .000   1000.000
    12.000      3.000       .000    11.200     14.000  -48.91131     -1.000     10.000
    41     21      0     10     -1     41     49     61     32      0     -1     -1     10      0    -21     13


Case 2: Ideal gas design, supersonic contour.
I-Gas-2          0
     1.4073  1716.563      1.000      .896  0.227E-07       .000       .000   1000.000
    12.000      3.000       .000    11.200     14.000    .00000       .000     10.000
    41     21      0     10      0     41     49     61     32      0     -1      0     10      0    -21     13
*input data for running inviscid design only.
```

Table A2. Subsonic contour

x	y_k	y_k'
-4.9462	4.2087	-1.0000
-4.8472	4.1098	-0.9996
-4.7483	4.0109	-0.9984
-4.6494	3.9123	-0.9963
-4.5505	3.8138	-0.9934
-4.4515	3.7158	-0.9897
-4.3526	3.6181	-0.9851
-4.2537	3.5209	-0.9796
-4.1548	3.4243	-0.9732
-4.0559	3.3284	-0.9659
-3.9569	3.2332	-0.9578
-3.8580	3.1389	-0.9487
-3.7591	3.0455	-0.9387
-3.6602	2.9532	-0.9278
-3.5612	2.8620	-0.9160
-3.4623	2.7720	-0.9033
-3.3634	2.6833	-0.8897
-3.2645	2.5960	-0.8752
-3.1655	2.5102	-0.8598
-3.0666	2.4259	-0.8435
-2.9677	2.3433	-0.8263
-2.8688	2.2625	-0.8082
-2.7699	2.1835	-0.7893
-2.6709	2.1064	-0.7695
-2.5720	2.0313	-0.7489
-2.4731	1.9582	-0.7275
-2.3742	1.8873	-0.7053
-2.2752	1.8187	-0.6823
-2.1763	1.7524	-0.6585
-2.0774	1.6885	-0.6340
-1.9785	1.6270	-0.6088
-1.8795	1.5680	-0.5829
-1.7806	1.5117	-0.5563
-1.6817	1.4580	-0.5291
-1.5828	1.4070	-0.5013
-1.4838	1.3588	-0.4729
-1.3849	1.3135	-0.4439
-1.2860	1.2710	-0.4144
-1.1871	1.2315	-0.3845
-1.0882	1.1950	-0.3540
-0.9892	1.1615	-0.3232
-0.8903	1.1310	-0.2920
-0.7914	1.1037	-0.2604
-0.6925	1.0795	-0.2286
-0.5935	1.0585	-0.1964
-0.4946	1.0407	-0.1640
-0.3957	1.0261	-0.1315
-0.2968	1.0147	-0.0987
-0.1978	1.0065	-0.0659
-0.0989	1.0016	-0.0330
0.0000	1.0000	0.0000

American Institute of Aeronautics and Astronautics

Table A3. Cases 1 and 2, supersonic contour

	Case 1			Case 2	
x^*	y_-	y_-'	x	y_-	y_-'
0.0000	1.0000	0.0000	0.0000	1.0000	0.0000
0.0434	1.0003	0.0145	0.0442	1.0003	0.0147
0.0882	1.0013	0.0291	0.0900	1.0013	0.0296
0.1345	1.0030	0.0438	0.1373	1.0031	0.0446
0.1823	1.0054	0.0584	0.1861	1.0056	0.0594
0.2316	1.0086	0.0724	0.2366	1.0090	0.0736
0.2828	1.0127	0.0854	0.2890	1.0132	0.0867
0.3360	1.0176	0.0975	0.3435	1.0182	0.0987
0.3916	1.0233	0.1085	0.4004	1.0242	0.1098
0.4499	1.0299	0.1188	0.4603	1.0311	0.1201
0.5115	1.0375	0.1284	0.5235	1.0390	0.1297
0.5769	1.0462	0.1375	0.5908	1.0480	0.1387
0.6467	1.0561	0.1460	0.6627	1.0583	0.1472
0.7215	1.0674	0.1541	0.7399	1.0700	0.1552
0.8022	1.0801	0.1617	0.8232	1.0832	0.1628
0.8894	1.0946	0.1689	0.9134	1.0982	0.1698
0.9842	1.1109	0.1755	1.0116	1.1153	0.1764
1.0873	1.1293	0.1817	1.1187	1.1345	0.1825
1.2000	1.1501	0.1873	1.2360	1.1562	0.1881
1.3233	1.1735	0.1925	1.3647	1.1808	0.1931
1.4587	1.1999	0.1970	1.5064	1.2085	0.1976
1.5062	1.2093	0.1983	1.5553	1.2182	0.1989
1.5753	1.2231	0.2001	1.6265	1.2324	0.2006
1.6556	1.2392	0.2020	1.7095	1.2491	0.2024
1.7441	1.2572	0.2037	1.8012	1.2677	0.2041
1.8395	1.2767	0.2053	1.8999	1.2880	0.2056
1.9406	1.2975	0.2068	2.0048	1.3096	0.2070
2.0469	1.3196	0.2080	2.1153	1.3326	0.2082
2.1581	1.3428	0.2091	2.2310	1.3567	0.2092
2.2737	1.3670	0.2100	2.3515	1.3820	0.2101
2.3935	1.3922	0.2107	2.4767	1.4083	0.2108
2.5174	1.4183	0.2112	2.6062	1.4357	0.2113
2.6450	1.4453	0.2117	2.7399	1.4639	0.2117
2.7762	1.4731	0.2120	2.8776	1.4931	0.2120
2.9109	1.5017	0.2122	3.0192	1.5231	0.2122
3.0486	1.5309	0.2124	3.1643	1.5540	0.2124
3.1894	1.5608	0.2125	3.3127	1.5855	0.2125
3.3328	1.5913	0.2125	3.4643	1.6177	0.2125
3.4788	1.6223	0.2125	3.6188	1.6505	0.2125
3.6269	1.6538	0.2125	3.7758	1.6839	0.2125
3.7771	1.6858	0.2126	3.9353	1.7178	0.2126
4.2585	1.7881	0.2126	4.2743	1.7899	0.2126
4.7757	1.8980	0.2126	4.6288	1.8652	0.2126
20.2481	5.1868	0.2126	22.2419	5.6090	0.2126
21.6287	5.4802	0.2126	23.1256	5.7968	0.2126
22.6561	5.6986	0.2126	23.4362	5.8624	0.2125
22.9710	5.7651	0.2125	23.7374	5.9264	0.2125
23.2764	5.8300	0.2125	24.0346	5.9895	0.2125
23.5777	5.8939	0.2125	24.3264	6.0517	0.2125
23.8735	5.9570	0.2125	24.6149	6.1131	0.2125
24.1659	6.0192	0.2125	24.8994	6.1734	0.2125
24.4542	6.0803	0.2125	25.1792	6.2328	0.2125
24.7378	6.1405	0.2125	25.4566	6.2916	0.2125
25.0188	6.2001	0.2125	25.7300	6.3498	0.2125
25.2958	6.2591	0.2125	26.0017	6.4076	0.2125
25.5711	6.3176	0.2125	26.2704	6.4649	0.2125
25.8434	6.3757	0.2125	26.5384	6.5218	0.2124
26.1149	6.4333	0.2124	26.8053	6.5782	0.2124
26.3852	6.4905	0.2124	27.0704	6.6346	0.2124
26.6537	6.5475	0.2124	27.3365	6.6909	0.2123
26.9232	6.6046	0.2123	27.6019	6.7474	0.2123
27.1920	6.6619	0.2123	27.8696	6.8042	0.2122
27.4631	6.7194	0.2122	28.1379	6.8614	0.2121
27.7348	6.7773	0.2121	28.4098	6.9190	0.2120
28.0103	6.8356	0.2120	28.6847	6.9771	0.2119
28.2887	6.8944	0.2119	28.9623	7.0359	0.2118
28.5698	6.9539	0.2118	29.2454	7.0957	0.2117
28.8566	7.0146	0.2116	29.5327	7.1566	0.2115
29.1476	7.0763	0.2115	29.8271	7.2188	0.2113
29.4459	7.1393	0.2113	30.1271	7.2824	0.2111
29.7499	7.2038	0.2111	30.4360	7.3476	0.2109
30.0629	7.2697	0.2108	30.7533	7.4142	0.2106
30.3845	7.3372	0.2106	31.0784	7.4826	0.2103
30.7139	7.4066	0.2103	31.4149	7.5532	0.2100
31.0550	7.4781	0.2100	31.7607	7.6259	0.2097
31.4057	7.5519	0.2097	32.1198	7.7011	0.2093
31.7698	7.6282	0.2093	32.4898	7.7788	0.2089
32.1452	7.7070	0.2089	32.8749	7.8591	0.2085
32.5359	7.7882	0.2084	33.2740	7.9419	0.2080
32.9408	7.8723	0.2080	33.6865	8.0277	0.2076
33.3595	7.9593	0.2075	34.1161	8.1166	0.2070
33.7957	8.0497	0.2069	34.5608	8.2088	0.2065
34.2472	8.1433	0.2064	35.0241	8.3044	0.2058
34.7178	8.2403	0.2057	35.5053	8.4031	0.2052
35.2067	8.3404	0.2051	36.0028	8.5050	0.2045
35.7122	8.4439	0.2044	36.5208	8.6106	0.2038
36.2386	8.5512	0.2037	37.0558	8.7197	0.2031
36.7825	8.6621	0.2029	37.6119	8.8325	0.2023
37.3481	8.7768	0.2021	38.1872	8.9485	0.2015
37.9331	8.8944	0.2013	38.7795	9.0675	0.2006
38.5355	9.0154	0.2005	39.3919	9.1899	0.1997
39.1586	9.1399	0.1996	40.0204	9.3154	0.1988
39.7981	9.2676	0.1986	40.6676	9.4440	0.1979
40.4569	9.3982	0.1977	45.5936	10.4010	0.1909
45.4064	10.3586	0.1906	51.1211	11.4361	0.1833
50.9606	11.3969	0.1831	57.1825	12.5233	0.1757
57.0427	12.4870	0.1755	63.7315	13.6489	0.1681
63.6160	13.6157	0.1679	70.7395	14.8003	0.1606
70.6486	14.7690	0.1604	78.1784	15.9672	0.1533
78.1120	15.9386	0.1532	86.0418	17.1442	0.1463
86.0005	17.1183	0.1461	94.3054	18.3253	0.1395
94.2893	18.3019	0.1394	102.9725	19.5057	0.1330
102.9817	19.4847	0.1329	112.0193	20.6811	0.1268
112.0539	20.6624	0.1267	121.4564	21.8485	0.1209
121.5164	21.8319	0.1208	131.2586	23.0049	0.1152
131.3438	22.9902	0.1151	141.4433	24.1482	0.1097
141.5538	24.1353	0.1096	151.9816	25.2767	0.1045
152.1173	25.2653	0.1044	162.8970	26.3891	0.0994
163.0581	26.3792	0.0994	174.1545	27.4819	0.0946
174.3409	27.4757	0.0945	185.7686	28.5519	0.0900
185.9790	28.5469	0.0900	197.7578	29.6024	0.0856
197.9927	29.5983	0.0856	210.0754	30.6341	0.0813
210.3356	30.6307	0.0813	222.7398	31.6348	0.0773
223.0232	31.6349	0.0772	235.7802	32.6140	0.0733
236.0874	32.6145	0.0733	249.1334	33.5711	0.0695
249.4654	33.5751	0.0695	262.8302	34.4950	0.0659
263.1840	34.4991	0.0659	276.8999	35.3995	0.0624
277.2779	35.4032	0.0624	291.2696	36.2683	0.0591
291.6692	36.2755	0.0591	305.9769	37.1161	0.0558
306.3995	37.1225	0.0558	321.0083	37.9297	0.0527
321.4524	37.9395	0.0527	336.4212	38.7176	0.0497
336.8876	38.7263	0.0497	352.1075	39.4723	0.0468
352.5946	39.4842	0.0468	368.1229	40.2038	0.0440
368.6320	40.2140	0.0440	384.4501	40.8966	0.0414
384.9785	40.9100	0.0414	401.1570	41.5690	0.0387
401.7081	41.5802	0.0387	418.1177	42.1969	0.0363
418.6861	42.2112	0.0363	435.3822	42.8081	0.0338
435.9726	42.8255	0.0338	452.9600	43.3789	0.0316
453.5676	43.3934	0.0316	470.8254	43.9230	0.0293
471.4521	43.9405	0.0293	489.0757	44.4382	0.0271
489.7224	44.4522	0.0271	507.5352	44.9135	0.0251
508.1975	44.9304	0.0251	526.2770	45.3713	0.0231
526.9596	45.3910	0.0231	545.3119	45.7915	0.0212
546.0105	45.8072	0.0212	564.6076	46.1803	0.0194
565.3219	46.1987	0.0194	584.1759	46.5515	0.0176
584.9110	46.5724	0.0176	604.1151	46.8727	0.0159
604.8627	46.8891	0.0159	624.2008	47.1758	0.0143
624.9637	47.1947	0.0143	644.5425	47.4616	0.0128
645.3256	47.4812	0.0127	665.1430	47.7112	0.0113
665.9414	47.7286	0.0113	685.9780	47.9320	0.0099
686.7911	47.9489	0.0099	707.0390	48.1267	0.0086
707.8662	48.1432	0.0086	728.3163	48.2959	0.0073
729.1577	48.3122	0.0073	749.8015	48.4407	0.0062
750.6555	48.4568	0.0061	771.4825	48.5622	0.0051
772.3491	48.5782	0.0051	793.3483	48.6619	0.0041
794.2269	48.6777	0.0040	815.3859	48.7410	0.0031
816.2759	48.7564	0.0031	837.5809	48.8012	0.0023
838.4818	48.8163	0.0023	859.9172	48.8442	0.0016
860.8279	48.8591	0.0016	882.3756	48.8723	0.0010
883.2954	48.8871	0.0009	904.9333	48.8882	0.0005
905.8615	48.9028	0.0005	927.5628	48.8951	0.0002
928.4987	48.9096	0.0002	950.2318	48.8968	0.0000
951.1747	48.9112	0.0000	972.9101	48.8968	0.0000
973.8597	48.9113	0.0000			

x^*, already shifted from source reference by 4.1537.

8